

Nanoscale

Accepted Manuscript

This article can be cited before page numbers have been issued, to do this please use: M. J. Islam, L. Ontiveros-Padilla, S. A. Ehrenzeller, D. D. Middleton, J. Roque III, C. Murphy, N. R. Lukesh, D. Hendy, E. S. Pena, R. Stack, W. J. Polacheck, E. M. Bachelder and K. Ainslie, *Nanoscale*, 2026, DOI: 10.1039/D5NR03936C.



This is an Accepted Manuscript, which has been through the Royal Society of Chemistry peer review process and has been accepted for publication.

Accepted Manuscripts are published online shortly after acceptance, before technical editing, formatting and proof reading. Using this free service, authors can make their results available to the community, in citable form, before we publish the edited article. We will replace this Accepted Manuscript with the edited and formatted Advance Article as soon as it is available.

You can find more information about Accepted Manuscripts in the [Information for Authors](#).

Please note that technical editing may introduce minor changes to the text and/or graphics, which may alter content. The journal's standard [Terms & Conditions](#) and the [Ethical guidelines](#) still apply. In no event shall the Royal Society of Chemistry be held responsible for any errors or omissions in this Accepted Manuscript or any consequences arising from the use of any information it contains.

A Novel Manganese Glycerophosphate Vaccine Gel Elicits Broad and Durable Immunity

Across an Aged and Pox Virus Model

Md Jahirul Islam¹, Luis Ontiveros-Padilla¹, Stephen A. Ehrenzeller¹, Denzel D. Middleton¹, John A. Roque III¹, Connor T. Murphy¹, Nicole Rose Lukesh¹, Dylan A. Hendy¹, Erik S. Pena^{1,2}, Ryan N. Stack³, William J. Polacheck³, Eric M. Bachelder¹,
Kristy M. Ainslie^{1,2,4*}

¹Division of Pharmacoengineering and Molecular Pharmaceutics, Eshelman School of Pharmacy, University of North Carolina at Chapel Hill, Chapel Hill, North Carolina, USA

²Joint Department of Biomedical Engineering, University of North Carolina at Chapel Hill and North Carolina State University, Chapel Hill, North Carolina, USA

³Lampe Joint Department of Biomedical Engineering, University of North Carolina at Chapel Hill and North Carolina State University, Chapel Hill, North Carolina, USA.

⁴Department of Microbiology & Immunology, UNC School of Medicine, University of North Carolina at Chapel Hill, Chapel Hill, North Carolina, USA.

¹ ^ Authors contributed equally

*Corresponding author: ainsliek@email.unc.edu

Keywords: Manganese glycerophosphate gel, long-lasting antibody response, memory T cell response, subunit vaccine,

Orthopoxvirus, aged mice.



ABSTRACT:

Subunit vaccines, composed of a protein antigen and an adjuvant, offer a safer and more versatile strategy than traditional live-attenuated vaccines, but limitations of conventional adjuvants like alum require improved design and delivery. Manganese (Mn) has emerged as a novel adjuvant that stimulates the cGAS-STING pathway, showing profound pre-clinical efficacy in vaccines against infectious diseases and cancer, but its potential dose-limiting toxicities require innovative delivery strategies. Herein, we report the development of gel derived from the generally recognized as safe (GRAS) material manganese glycerophosphate (MnGp). The gel displayed tunable controlled antigen release based on MnGp concentration that activated dendritic cells (DCs) *in vitro*, eliciting substantial production of type I interferons and upregulation of costimulatory markers. A single immunization of mice with ovalbumin (OVA) and 250 mg/mL MnGp gel generated the highest and most durable OVA-specific total IgG, IgG1, and IgG2c serum antibody titers. Subsequently, a prime-boost-boost immunization with 250 mg/mL MnGp gel elicited a long-lasting OVA-specific IgG, IgG1, and IgG2c sera antibody response and it was superior to MF59-mimic AddaVax and STING agonists 2,3-cGAMP. Splenocytes from mice immunized with MnGp secreted high levels of Th1-associated cytokines upon antigen recall and illustrated generation of memory CD4⁺ and CD8⁺ T cells. Immunizing MnGp in 18-month-old mice elicited superior IgG and IgG1 antibody titers compared to Addavax, in addition to specific T cell responses in spleen and the draining lymph node. Finally, the co-immunization of MnGp and B5R (a vaccinia virus protein) induced higher B5R-specific antibody titers than Addavax and achieved full protection against the challenge with vaccinia virus. Overall, these findings corroborate the potential for MnGp gels as a novel vaccine platform.



38 **INTRODUCTION:**

39 Vaccination stands as one of the most successful public health measures to date with the worldwide eradication
40 of Smallpox in 1980 as a shining example of this effort.[1, 2] Smallpox, caused by *Variola major* and *V. minor*, is responsible
41 of the death of an estimated 10% of the human population over thousands of years, including 300–500 million deaths in
42 the 20th century alone. Despite its eradication, smallpox remains a critical bioterrorism threat, and outbreaks of related
43 *Orthopoxviruses* (e.g., monkeypox (mPox)) continue to pose public health risks due to zoonotic transmission.[3, 4] In
44 November 2022, the WHO reported over 78,000 cases of monkeypox with more than 98% occurring in non-endemic
45 regions. This unprecedented spread prompted the WHO to declare the outbreak a Public Health Emergency of
46 International Concern. [5, 6]. In response to the outbreak, the Bavarian-Nordic vaccine, JYNNEOS, was distributed to those
47 deemed at high-risk for mPox exposure. JYNNEOS received an Emergency Use Authorization (EUA) by the FDA, which
48 allowed for intradermal administration and subsequent dose-sparing. While this significantly slowed the spread of disease,
49 the protection elicited by the JYNNEOS vaccine has been shown to quickly wane, as the vaccine generates sub-optimal
50 quantities of neutralizing antibodies.[7] JYNNEOS also contains a live-attenuated, non-replicating vaccinia virus, which is
51 considerably safer than the replication-competent strain used in the older ACAM2000 vaccine. However, some safety
52 concerns remain, particularly for immunocompromised populations. [8].

53 With the available mPox vaccines, a broad vaccination strategy for the general public would be limited since it
54 does not take into consideration high-risk individuals, such as those who are living with HIV and would have compromised
55 immunity.[9, 10] Vaccine development to protect high-risk populations is gaining attention recently due to the SARS-CoV-
56 2 mRNA vaccine, which demonstrated profound efficacy in preventing severe illness and improving disease outcomes in
57 aged, immunocompromised, and high-risk comorbidity populations.[11-13] Nevertheless, complications observed with
58 the mRNA vaccine rollout and global distribution (e.g. poor stability outside of cold-chain storage) and carrier-mediated
59 reactogenicity,[14, 15] highlight the continual need to develop novel vaccine formulations for high-risk populations.

60 Traditional vaccine development is largely focused on the production of live attenuated pathogens, but the
61 capacity for vaccine strains to replicate in and cause illness to the host prompts safety concerns for immunocompromised
62 populations.[16, 17] In contrast, subunit vaccines, composed of purified proteins, peptides, or polysaccharides from a
63 pathogen, are noninfectious and offer a promising alternative that avoids these safety concerns.[18] Because subunit



antigens are weakly immunogenic and typically induce only modest humoral responses with little to no cellular immunity, subunit vaccines often include adjuvants to enhance and sustain the immune response.[19] Aluminum-containing adjuvants (i.e., alum) are perhaps the most widely used subunit vaccine adjuvants, largely due to their potency, safety profile, and relatively accessible cost.[20] However, despite proven efficacy in several licensed vaccines, alum primarily elicits a T helper 2 (Th2) cell-biased response (i.e., antibody-mediated, or humoral immunity) with a marginal T helper 1 (Th1) cell response (i.e., cell-mediated immunity).[21] Thus, for diseases where a robust Th1 response is critical, such as influenza and certain cancers,[22, 23] candidate vaccines require more effective adjuvant systems. As such, significant progress has been made in the exploration of depot-forming emulsion systems like MF59, adjuvant system 01 (AS01) and AS03.[24-26] Further, there is a greater development for agonist which stimulate pattern recognition receptors such as toll-like receptor (TLR) agonists (e.g., poly(I:C), CpG), and cyclic GMP-AMP synthase (cGAS)-stimulator of interferon genes (STING) agonists (e.g., cGAMP) to invoke a Th1 vaccine responses.[27-29]

Manganese (Mn) is an emerging adjuvant that possesses varied effects on the cGAS-STING pathway.[30-33] Classically, the cGAS-STING pathway orchestrates the immunological responses to double-stranded DNA (dsDNA). Upon binding dsDNA, cGAS catalyzes the synthesis of the second messenger cyclic GMP-AMP (cGAMP), which subsequently binds and activates STING. Activated STING then initiates a number of downstream processes, ultimately resulting in the expression of type I interferons and several interferon-stimulated genes that regulate the anti-viral immune response.[34] Interestingly, Mn(II) has been found to augment cGAS-STING through both DNA-dependent and DNA-independent mechanisms. Manganese was first discovered to modulate the sensitivity of cGAS-STING to dsDNA, as Mn-deficient WT mice demonstrated increased susceptibility to dsDNA, but not RNA, viruses in a STING-dependent manner.[31] Alternatively, manganese has since been shown to directly activate cGAS to synthesize cGAMP,[33] as well as to associate with cGAMP to enhance cGAMP-STING binding affinity.[31] Given these mechanisms, several groups have already investigated the adjuvanticity of manganese to augment anti-tumor and anti-viral responses with substantial success.[30, 35]

To enhance delivery of manganese to target immune cells, these adjuvants have largely been encapsulated in or formulated as nanoparticles.[36-41] Although improved compared to soluble injections of Mn, many of these formulation strategies require sophisticated fabrication processes that are poorly scalable. Furthermore, nanoparticles often offer



90 limited antigen/adjuvant dosing and are rapidly cleared from the injection site. In contrast, gel-based delivery systems
91 offer several potential advantages that address the limitations of nanoparticle-based formulations. Foremost, many gel-
92 like formulations exhibit shear thinning behavior, characteristic of pseudoplastic or thixotropic materials, which allows
93 them to form a well-defined and long-lasting depot upon injection. Given that several adjuvant systems, including
94 nanoparticles, exploit this phenomenon to prolong immune responses,[42] developing a gel-based formulation for
95 manganese could further enhance antigen and adjuvant retention and controlled release at the injection site, while also
96 acting as a cGAS-STING agonist to potentially elicit a stronger and more sustained immune response. Furthermore,
97 depending on the chemistries, gels can be highly scalable, thermostable, and optimized for a wider range of administration
98 profiles (e.g., mucosal, intradermal).[43] Therefore, a gel-based formulation for Mn-adjuvanted vaccines represents a
99 promising yet underexplored strategy to improve vaccination.

100 Herein, we report the fabrication and characterization of a novel gel derived from manganese glycerophosphate
101 (MnGp), hereafter referred to as an MnGp gel. The US FDA recognizes manganese glycerophosphate as a generally
102 regarded as safe (GRAS) material, underscoring the potential safety of our gel formulation. Compared to typical polymeric
103 initiators used in the fabrication of gel-based drug delivery formulations, MnGp was selected as the gel precursor as it
104 bypasses the need for adjuvant encapsulation or chemical ligation, thereby circumventing a potentially limiting design
105 consideration and instilling the delivery system with inherent adjuvanticity. Following the development of a facile and
106 scalable fabrication method, MnGp gels were first assessed for antigen release kinetics and *in vitro* activation of relevant
107 immune cell populations at a range of concentrations. Subsequently, we evaluated the potential for MnGp to act as
108 vaccine platforms *in vivo*. We characterized the dosing, immunization schedules, humoral and cellular immunity and the
109 protection induced by this platform against the *Orthopoxvirus* vaccinia. Finally, we immunized MnGp in an aged mice
110 model to assessed the immune response induced by this vaccine in a high-risk group of vaccination.



METHODS:Materials:

Unless otherwise specified, all chemicals were purchased and used unmodified from Sigma Aldrich (St. Louis, MO) and all assays, biologics, and disposables were purchased from ThermoFisher Scientific (Waltham, MA). Separately, commercial adjuvants (Addavax, CpG, cGAMP) were acquired from Invivogen (San Diego, CA).

Preparation and Characterization of MnGp Gels:

A dry mixture of MnGp (Pfaltz & Bauer; Waterbury, CT) and sucrose was resuspended to 350 mg/mL MnGp and 150 mg/mL sucrose in 0.1M HEPES. The suspension was then placed in an ice bath and probe sonicated (Q500 Sonicator; QSonica Sonicators; Newtown, CT) for 30 minutes (1 second on, 1 second off) at maximum amplitude (100%). After sonication, the resultant gel was stored at 4°C until use. Endotoxin level was confirmed to be less than 0.1 EU/dose using a limulus amoebocyte lysate-based assay.

MnGp gels were imaged using scanning electron microscopy (SEM; Hitachi S-4700 Cold Cathode Field Emission; Ibaraki, Japan; UNC CHANL). To prepare samples, a droplet of the MnGp gel was spread on an SEM sample mount affixed with adhesive carbon tape. The mount was then submerged in liquid nitrogen for 1 minute and lyophilized for at least 48 hours prior to imaging.

The viscosity characterization of Mn-Gp gels was performed using Discovery HR-20 rheometer (TA Instruments) with a 20 mm diameter parallel plate geometry (100-110 μm). A frequency sweep test was performed at 20° C with shear rate ranging from 0.0001 to 1000 (1/s) using logarithmic sampling (5 points/decades). Shear thinning behavior was quantified using the Ostwald–de Waele power-law model, expressed in viscosity from as:

$$\eta = K \left(\frac{du}{dy} \right)^{n-1}$$

Assessment of OVA Release from MnGp Gels:

5, 25, 100 and 250 mg/mL MnGp gels were prepared via dilution of the stock 350 mg/mL MnGp gel in 0.1 M HEPES and subsequently loaded with OVA protein (Fisher Scientific; New Hampton, NH) via mixing. To measure OVA release from



135 the MnGp gels, 50 μ L of the OVA-loaded MnGp gels were dispensed into 96-well plates and layered with 200 μ L PBS, with
136 three wells prepared for each timepoint. At each timepoint, the plates were centrifuged at 500 x g for 5 minutes, and the
137 supernatant was collected and stored at 4°C prior to analysis. OVA content in the supernatant was quantified using a
138 Bradford's assay following the manufacturer's protocol. Percent release was quantified as the amount of OVA present in
139 the supernatant relative to the known OVA content initially loaded in each gel aliquot.

140 Cell Culture and Treatments:

141 All experiments involving mice were performed with the approval of the University of North Carolina at Chapel
142 Hill Institutional Animal Care and Use Committee (IACUC). Bone marrow-derived dendritic cells (BMDCs) were
143 differentiated from murine bone marrow as previously described.[44-46] In short, C57BL/6J mice (Jackson Laboratory; Bar
144 Harbor, ME) were humanely euthanized and bone marrow was collected from the femurs and tibias. The bone marrow-
145 derived cells were then cultured in Roswell Park Memorial Institute 1640 medium (RPMI 1640; Corning; Corning, NY)
146 supplemented with 10% heat-inactivated fetal bovine serum (FBS; Corning), 1% penicillin-streptomycin solution (Corning),
147 and 10 ng/mL GM-CSF for 10 days, followed by RPMI 1640 supplemented with 10% heat-inactivated FBS, 1% penicillin-
148 streptomycin solution, 10 ng/mL GM-CSF, and 10 ng/mL IL-4 for the next 4 days. After the 14-day culture, cells were
149 immediately used for cell-based assays.

150 To assess the immunostimulatory properties of the MnGp gel, BMDCs were cultured with the MnGp gel in a
151 transwell model. The bottom of a 12-well transwell plate was first pre-coated with the 100 mg/mL MnGp gel, and BMDCs
152 were then plated at 1×10^5 cells/well in the upper transwell insert. Additional BMDCs were cultured in base media with
153 and without 100 ng/mL LPS. To determine changes in cell phenotype, cells were collected after 12 hours and stained with
154 eBioscience Fixable Viability Dye (eFluor 506; Fisher Scientific; New Hampton, NH) and the following fluorophore-
155 conjugated antibodies (Biolegend; San Diego, CA): MHC-II (FITC, clone: M5/114.15.2), CD86 (PE, clone: GL-1), CD80
156 (PE/Cy7, clone: 16-10A1), CD40 (APC/Cy7, clone: 3/23), CD11c (BV421, clone: N418), and CD11b (BV711, clone: M1/70).
157 To determine cytokine secretion levels, cell supernatants were collected after 24 hours and the concentration of IFN- β
158 was determined via ELISA (R & D Systems; Minneapolis, MN).

159 In Vivo Immunizations & Sample Collection:



160 For the initial MnGp gel titration studies, 6–8-week-old C57BL/6J mice (n=5 per group) were immunized
161 intramuscularly on day 0 with saline, soluble OVA (25 µg per mouse), OVA + AddaVax, OVA + 5 mg/mL MnGp gel, OVA +
162 25 mg/mL MnGp gel, OVA + 100 mg/mL MnGp gel, or OVA + 250 mg/mL MnGp gel. Mice were dosed at 25 µL per hind
163 limb (50 µL total) and 25 µg of endotoxin-free OVA (Invivogen; San Diego, CA. AddaVax formulations were prepared via
164 1:1 v/v mixing of AddaVax (Invivogen) with OVA according to the manufacturer's protocol. MnGp gel formulations were
165 prepared as described for the OVA release studies. Submandibular bleeds were subsequently collected biweekly through
166 week 18 (day 126).

167 For subsequent immunization studies, 6-8 week old C57BL/6J mice (n=5) were immunized intramuscularly on days
168 0, 28 and 140 with saline, soluble OVA (25 µg per mouse), OVA + AddaVax, OVA + 2,3-cGAMP (1 µg), OVA + 250 mg/mL
169 MnGp, or OVA + 250 mg/mL MnGp + 2,3'-cGAMP (0.01, 0.1, or 1 µg). Mice were boosted on day 140 to stimulate cellular
170 responses. Submandibular bleeds were collected biweekly through week 18 (day 126), as well as 10 days following the
171 final boost (day 150). On day 151, mice were humanely euthanized to collect spleens and draining lymph nodes (dLNs),
172 which were subsequently processed into single cell suspensions as previously described.[47]

173 For the aged mice study, 18 month-old C57BL/6J mice (n=5) were obtained from the National of Institute of Aging
174 and were immunized intramuscularly on days 0 and 28 as described above with PBS, OVA (25 µg per mouse) , 250 mg/mL
175 MnGp + OVA (1:1 v/v and 25 µg) or Addavax + OVA (1:1 v/v and 25 µg). Submandibular bleeds were collected biweekly
176 and on day 77 mice were homologous boosted to evaluate the cellular immune response. On day 84, spleens were
177 harvested and processed into single cell suspensions as previously described.

178 Challenge study:

179 6–8-week-old BALB/c mice (n=10) were immunized intramuscularly on days 0 and 28 as described above with PBS,
180 CpG + B5R (10 µg each item per mouse), 250 mg/mL MnGp + B5R (1:1 v/v and 10 µg) or Addavax + B5R (1:1 v/v and 10
181 µg). Submandibular bleeds were collected biweekly until day 56 when each mouse was challenged intranasally with 5x10⁴
182 pfu of vaccinia virus (Western Reserve - NR-55). Survival and weight loss were monitored for 14 days after challenge. Mice
183 were also scored according to previous studies,[48] based on the presentation of the next clinical signs: 0 (normal), 1
184 (slightly ruffled fur), 2 (clearly ruffled fur), 3 (hunched posture and/or conjunctivitis with fur ruffling), and 4 (score of 3
185 combined with difficulty breathing/moving/socializing).



Determination of Antibody Titers:

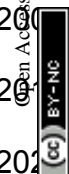
OVA-specific and B5R-specific antibody titers in the collected sera were determined by a previously described indirect ELISA method.[44, 49] Briefly, high-binding 384-well plates (Greiner Bio-One; Kremsmünster, Austria) were coated with OVA (10 $\mu\text{g}/\text{mL}$) or B5R (1 $\mu\text{g}/\text{mL}$) in PBS and incubated at 4°C overnight. Plates were then blocked with 3% w/v instant nonfat dry milk in PBS (blocking buffer; Food Lion; Salisbury NC) for 1 hour at room temperature (RT) and incubated with sera samples across a range of dilutions for 2 hours at RT. Plates were subsequently incubated with IgG, IgG1, and IgG2c-specific HRP-conjugated detection antibodies (Southern Biotech; Birmingham AL) for 30 minutes at RT. 3,3',5,5'-tetramethylbenzidine (TMB) was then added to initiate the detection reaction, and development was quenched with 2 N sulfuric acid. A minimum of three washes with 0.05% v/v Tween 20 in PBS (PBST) were performed between each step. Absorbances at 450 and 570 nm were read on a plate reader (SpectraMax M2 Microplate Reader; Molecular Devices; Sunnyvale, CA), with the 570 nm absorbance subtracted from the 450 nm absorbance to correct for background. Titer was determined using a plot of correct absorbance against serum dilution factor as previously reported.[50, 51]

Assessment of Antigen Recall:

Antigen recall was assessed by both ELISA and ELISPOT, as previously described.[44, 47, 49, 50] For ELISAs, splenocytes and dLN cells from immunized mice were plated at 1×10^6 cells per well in a 96-well plate and incubated with 10 $\mu\text{g}/\text{mL}$ OVA protein for 36 hours. After 36 hours, the cell supernatants were collected and stored at -80°C until use. IFN- γ , IL-4 and IL-2 content in the supernatants was measured via ELISA according to the manufacturer's protocol (Biolegend; San Diego, CA). For ELISPOTs, splenocytes from immunized mice were plated at 1×10^6 cells per well in a multi-screen-IP 0.45 μm filter 96-well plate (Sigma Aldrich; St. Louis, MO) pre-coated with the desired capture antibody. Cells were then incubated with 10 $\mu\text{g}/\text{mL}$ OVA protein for 36 hours, and ELISPOTs were developed according to the manufacturer's protocol (BD Biosciences; San Jose, CA). Spots were counted with the AID Classic ELISpot Reader (AID Autoimmun Diagnostika GmbH; Straßberg, Germany).

Immune Cell Phenotyping via Flow Cytometry:

Following generation of single cell suspensions from spleens, cells were stained to assess immune phenotype and OVA-specificity. To profile immune cell phenotypes, 1×10^6 cells were stained with eBioscience Fixable Viability Dye (eFluor



506) and the following fluorophore-conjugated antibodies (Biolegend; San Diego, CA): CD3 (AF488, clone: 17A2), CD4 (APC/Fire 750, clone: RM4-5), CD8 (PerCP/Cy5.5, clone: 53-6.7), CD44 (BV421, clone: IM7), CD62L (BV785, clone: MEL-14), CD19 (APC, clone: 6D5), GL7 (PE, clone: GL7), and CD38 (PE/Cy7, clone: 90). Tetramer staining to assess OVA-specificity was performed as a separate panel. In short, 1×10^6 cells were first incubated with 50 nM desatinib for 30 minutes at 37°C. Cells were subsequently stained with OVA Class I (AF568, clone: H2-Kb/SIINFELK), OVA Class II (BV421, clone: I-A(b)/AAHAEINEA), or control tetramers (clone: I-A(b)/PVSKMMRMATPLLMQA) acquired from the NIH Tetramer Facility at Emory University (Atlanta, GA). Cells were then stained with the following fluorophore-conjugated antibodies (Biolegend; San Diego, CA): CD3 (AF488, clone: 17A2), CD4 (APC/Fire 750, clone: RM4-5), and CD8 (PerCP/Cy5.5, clone: 53-6.7). Following staining, cells were fixed with 1% paraformaldehyde and analyzed with an Attune NxT flow cytometer (ThermoFisher Scientific; Waltham, MA; UNC Flow Core Facility). Analysis of flow data was performed with FlowJo v10.9.0.

Statistical Analysis:

Figures and statistical analyses were prepared with GraphPad Prism 10. For *in vitro* adjuvanticity experiments, all data were compared via ordinary one-way ANOVA with Tukey's multiple comparisons test. For *in vivo* kinetics of vaccination studies, in order to compare the data between groups and the different time points, all data were compared via ordinary two-way ANOVA with Tukey's multiple comparisons test.



RESULTS & DISCUSSION:*Synthesis and Characterization of the MnGp Gel*

Sonication has been previously reported to develop metallo gel and hydrogel platforms,[52-54] where pulsatile forces, local temperature changes, and aeration are hypothesized to facilitate cross-linking of the gel-forming reagents. We hypothesized that the sustained high-intensity sonication of a concentrated solution of MnGp would promote gelation via hydrogen bonding. More specifically, mechanical disruption of the MnGp salts in an aqueous environment likely forces hydration of the salts and/or salt aggregates, thereby coordinating MnGp molecules via shared hydrogen bonding with intercalating water molecules.[55] Additionally, we opted to incorporate sucrose into the formulation due to its known properties as both a gel stabilizer and cryoprotectant.[56]

In this case, we were able to successfully synthesize a MnGp gel via probe sonication on ice for 30 minutes (Figure 1A). Comparison of the gel mixture before and after sonication demonstrated a significant shift in fluidity and viscosity, as evidenced by the retention of MnGp gel at the top of an inverted scintillation vial (Figure 1B). SEM of a lyophilized MnGp gel revealed an irregular architecture with microporous layers. The structure showed two different pore sizes: Small pores of around 5-15 μm (approximately 30% of the total pores) and medium size pores of around 20-40 μm (approximately 70% of the total pores). All this data suggests that there could be significant fluid retention in the gel matrix (Figure 1C).

Interestingly, the same architecture was observed for MnGp gels prepared without sucrose (Figure S1), suggesting that interactions between manganese glycerophosphate and water are the primary cross-linking mechanisms. For the same reason, its degradation is expected to occur primarily through ionic exchange and coordination bond dissociation under physiological conditions.



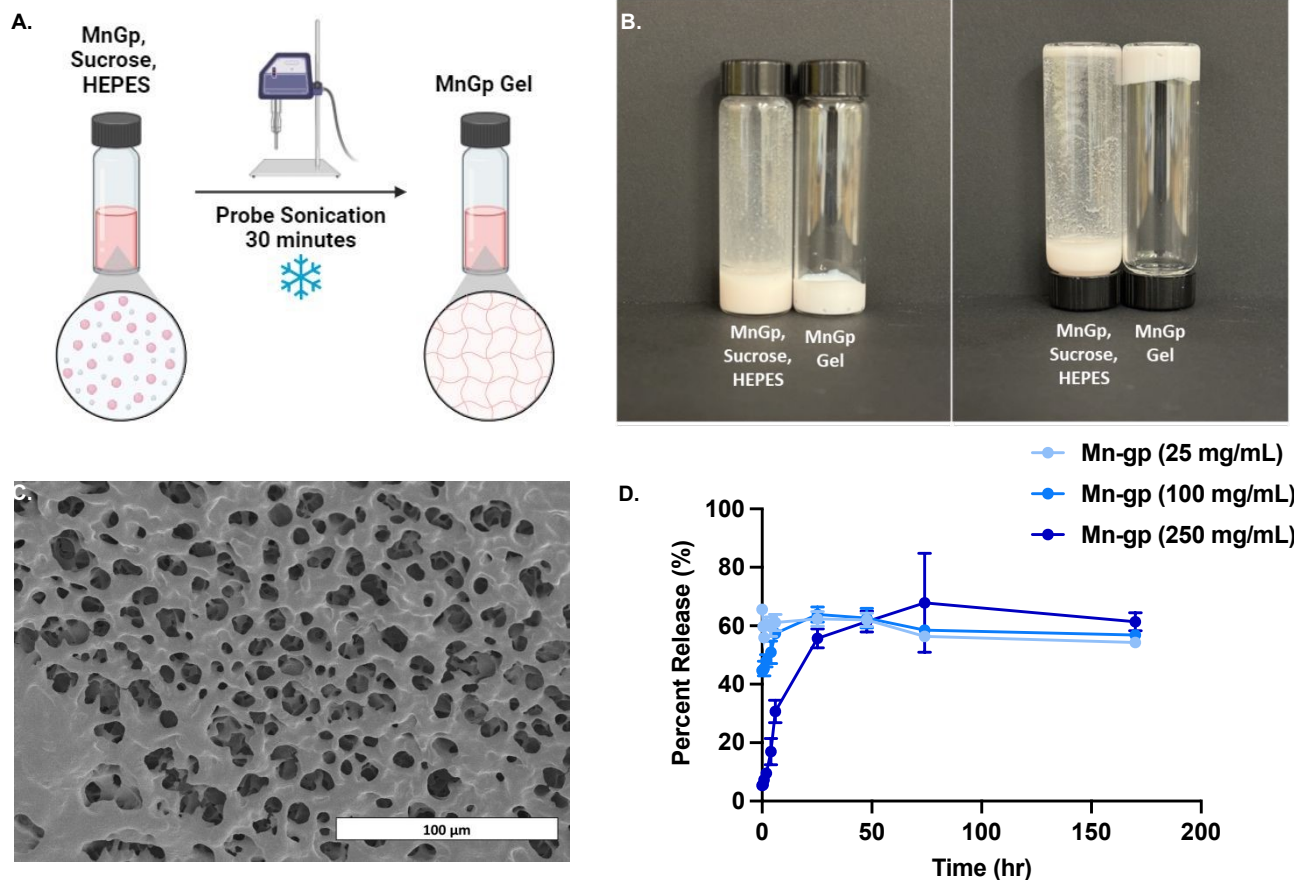


Figure 1. Synthesis and characterization of MnGp gel. **(A)** Synthesis schematic of MnGp gel. A concentrated solution of MnGp (350 mg/mL) and sucrose (150 mg/mL) in 0.1 M HEPES was probe sonicated for 30 minutes on ice, yielding the MnGp gel. **(B)** Comparison of the pre-sonication gel mixture (left) and resultant gel (right), with inverted containers documented to demonstrate fluidity and viscosity changes. **(C)** Scanning electron microscopy (SEM) image of the stock MnGp gel. **(D)** OVA-release by MnGp gels at various MnGp concentrations. The stock MnGp gel (350 mg/mL MnGp) was diluted to the indicated concentrations in 0.1M HEPES and loaded with OVA via vortexing. Release was monitored over 1 week at physiological conditions (pH 7.4, 37°C) and measured via Bradford's assay. Data is presented as mean \pm standard deviation (n=3).

Given the application of many gel-like materials as controlled release formulations, release of the model antigen OVA was measured from MnGp gels under physiological conditions (37°C, pH 7.4). OVA-loaded MnGp gels were prepared at various concentrations post-sonication by dilution of the stock gel in 0.1 M HEPES and simple mixing with OVA. The generated OVA release curves indicated clear concentration-dependent kinetics (Figure 1D). The 250 mg/mL MnGp gel had the slowest release, exhibiting a low burst release (around 5-10% percent of OVA) and approximately 60% of OVA released by 48 hours. The 100 mg/mL MnGp gel demonstrated slightly slowed kinetics, although burst release was nearly 50% and total release leveled off at around 60% OVA release after 24 hours. Both the 25 and 5 mg/mL MnGp gels exhibited no control over OVA release. These release kinetics aligned strongly with SEM of these gels, with increasing porosity and dispersity observed with decreasing concentration of MnGp. In addition, SEM analysis revealed concentration-dependent

265 microstructural transitions in the gels. Lower MnGp concentrations produced highly porous microporous networks,
266 consistent with lower cross-linking interactions and larger mesh size. Increasing MnGp concentration resulted in more
267 compact and homogeneous architectures, while intermediate concentrations displayed fibrillar structures, suggesting
268 diffusion-limited aggregation during gel formation (Figure S2A-C). The SEM of the OVA-loaded gel showed a change in the
269 gel structure (Figure S3), suggesting that some OVA protein might only interact on the surface, although according to our
270 release studies, the majority of the protein is loaded inside the gel.

271 Notably, no gels fully released their cargo, indicating that some OVA might be sequestered within the gel and
272 inaccessible to facile diffusion out of the gel matrix. It is important to note that *in vivo* release kinetics have not been
273 performed yet and it could be an important experiment to completely understand the behavior of this formulation. When
274 analyzing the rheological properties of the MnGp gel, we identified a shear thinning behavior, given the decrease in
275 viscosity as the shear rate increased and a value of the power-law index (n) of less than 1 (Figure S4). This is a highly
276 desired characteristic for adjuvant gels because enables it to be injected as a low viscosity, flowing material and to form a
277 stable long-lasting depot upon injection [57, 58].

279 *In Vitro Adjuvanticity of the MnGp Gel*

280 To determine the immunostimulatory properties of the MnGp gel, BMDCs were cultured with the 100 mg/mL MnGp
281 gel and assessed for relevant phenotypic changes and cytokine secretions (Figure 2A-D). As DCs are the primary innate
282 immune cell population involved in T cell education and activation, the response of DCs to the MnGp gel provides an early
283 insight into the potential efficacy of a vaccine platform. After 12 hours, the MnGp gel was well tolerated, with slight
284 reductions in cell viability observed compared to the untreated (UT) and LPS controls (Figure 2A); which can be explained,
285 as in previous reports, due to increased levels of cleaved-caspase 3 detected in cells stimulated with STING activators.[59]
286 MnGp gel treatment led to a marked upregulation of co-stimulatory molecules, with a significant increase in the frequency
287 of CD80⁺CD86⁺ cells (Figure 2B), and more than a twofold rise in the median fluorescence intensities (MFI) of CD80 (Figure
288 S5A) and CD86 (Figure S5B) compared to untreated cells. Furthermore, treatment with the MnGp gel resulted in a
289 considerable increase in MHC-II MFI (Figure 2C). Given that MHC-II is one of the molecules by which DCs present antigens
290 to T cells, and both CD80 and CD86 are co-stimulatory molecules involved in T cell activation, these data suggest that the



MnGp gel aptly poises DCs for presentation of antigen to T cells. Additionally, after 24 hours, there were significantly elevated levels of IFN- β in the cell supernatants of MnGp gel-treated cells compared to the untreated and LPS controls (Figure 2D), consistent with previous reports of manganese stimulating the cGAS-STING pathway.[32] Type I interferons such as IFN- β are also associated with improved T cell activation and differentiation into Th1-like phenotypes.[60] In the present study, IFN- β production was used as a functional downstream readout of pathway activation. Although upstream signaling intermediates (e.g., cGAS activation, STING translocation, TBK1/IRF3 phosphorylation) were not directly assessed, the increased IFN- β levels are consistent with activation of the canonical STING signaling cascade. However, this *in vitro* data further underscores the potential of the MnGp gel as a vaccine platform *in vivo*.

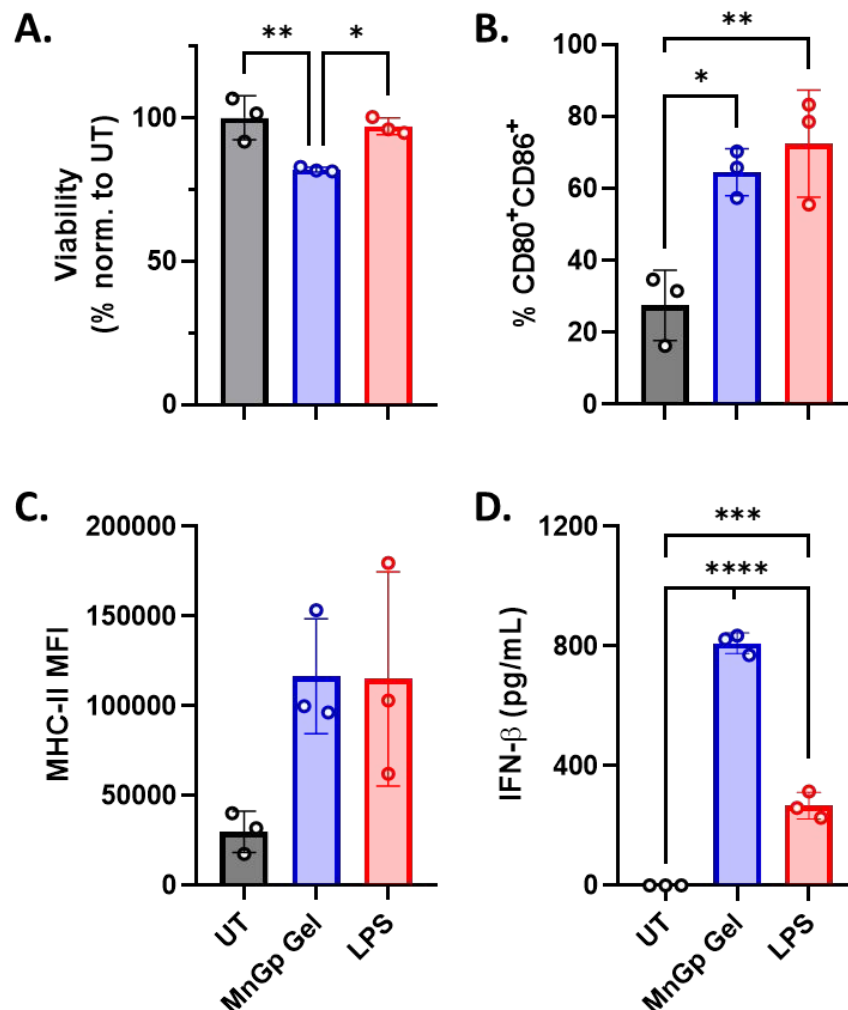


Figure 2. Activation of BMDCs by MnGp gel. BMDCs were cultured with media (UT), the 100 mg/mL MnGp gel, or 100 ng/mL LPS. **(A)** Normalized cell viability, **(B)** frequency of CD80⁺CD86⁺ cells, and **(C)** median fluorescence intensity (MFI) of MHC-II was assessed after 12 hours via flow cytometry. **(D)** IFN- β concentrations in the cell supernatants after 24 hours were measured via ELISA. Data is presented as mean \pm standard deviation (n=3). Statistical significance is presented as

291
292
293
294
295
296
297
298
299
300
301
302
303

Open Access Article. Published on 20 April 2026. Downloaded on 4/21/2026 11:11:06 AM.
This article is licensed under a Creative Commons Attribution-NonCommercial 3.0 Unported Licence.



*p<0.05, **p<0.01, ***p<0.001, and ****p<0.0001 for an ordinary one-way ANOVA with Tukey's multiple comparisons test.

In Vivo Titration of OVA-Loaded MnGp Gel Vaccine

Initial dose titration studies were performed to identify the optimal MnGp gel concentration for use as a vaccine platform. Mice were immunized once with saline, unadjuvanted OVA, OVA + AddaVax (analogous to FDA-approved adjuvant MF59), or OVA-loaded MnGp gels of increasing MnGp concentration, and sera were collected biweekly to measure OVA-specific IgG titers (Figure 3A-C). Total IgG titers exhibited concentration-dependent responses; wherein higher MnGp gel concentrations elicited superior titers (Figure 3A). Across all adjuvanted groups, total IgG titers peaked around 70 days post-immunization and subsequently decreased, with the 250 mg/mL MnGp gel inducing the highest and most sustained titers. It is reasonable that these results are due in part to concentration of manganese at the injection site, as well as the increased viscosity of the higher concentration MnGp gels since the same volume of gel was injected. The 250 mg/mL MnGp gel forms a well-defined, long-lasting depot in the intramuscular space, likely resulting in continued recruitment and activation of innate immune cells such as dendritic cells. IgG1 and IgG2c were additionally measured as markers of Th2 and Th1 responses, respectively.[61, 62] Both IgG1 (Figure 3B) and IgG2c (Figure 3C) titers mirrored the trends observed for total IgG, albeit at lower levels. Notably, the 100 and 250 mg/mL MnGp gels elicited significantly higher IgG2c titers compared to OVA adjuvanted with AddaVax at peak titers, suggesting that the MnGp gels might offer a more efficacious platform for inducing Th1 responses. Based on these data, 250 mg/mL MnGp was identified as the optimal formulation for further studies.



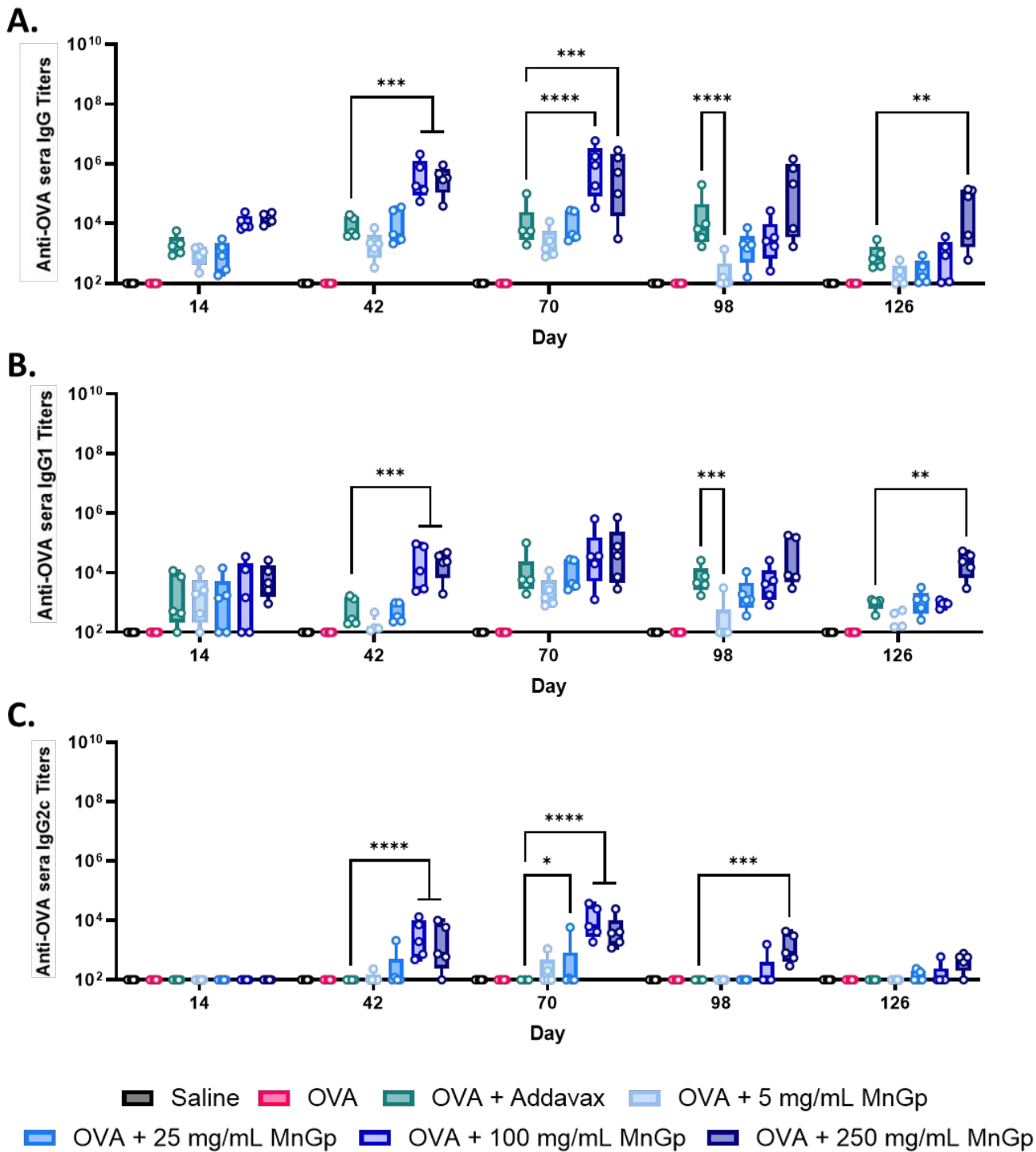


Figure 3. OVA-specific serum antibody titers following a single immunization. C57BL/6 mice ($n = 5$) were immunized intramuscularly on day 0 with saline, unadjuvanted OVA, OVA + Addavax, or OVA + the indicated concentrations of the MnGp gel. Sera were collected at the indicated timepoints and assessed for OVA-specific (A) total IgG, (B) IgG1, and (C) IgG2c titers via ELISA. Data is presented as median \pm range. Statistical significance is presented as * $p < 0.05$, ** $p < 0.01$, *** $p < 0.001$, and **** $p < 0.0001$ for an ordinary two-way ANOVA with Tukey's multiple comparisons test. Absence of statistical symbols indicates non-significant differences.



323

324

325

326

327

328

329

330

331

332

Humoral Response to Optimal OVA-Loaded MnGp Gel Vaccine

Initial concentration titration studies evaluated the durability of the humoral response following a single vaccination with OVA-loaded MnGp gel formulations. However, many vaccines often utilize sequential immunization, or boosts, to bolster immune memory and ensure long-term protection. Therefore, we sought to better characterize the immune response to the MnGp gel with a prime-boost schedule. Mice were immunized on days 0 and 28 with saline, unadjuvanted OVA, OVA + AddaVax, OVA + 250 mg/mL MnGp gel, or OVA + 2,3 cGAMP (an established STING agonist). An additional boost was performed on day 140 for subsequent cellular analyses. Also, given the ability of manganese to augment the cGAS-STING pathway, the 250 mg/mL MnGp gel was co-loaded with OVA and various doses of cGAMP to assess potential synergy.

As before, sera were collected biweekly and assessed for OVA-specific IgG titers (Figure 4A-C). Compared to a single immunization (Figure 3), boosting 28 days after the initial immunization yielded notably higher overall total IgG, IgG1, and IgG2c (Figure 4A-C) titers at subsequent timepoints. Titer kinetics additionally followed the same trend as with the prime-only vaccination, with titers initially peaking around day 70 and gradually decreasing thereafter for all IgG subtypes. Although trend was the same, the magnitude of response was significant with IgG and IgG1 titers remaining on average around 10^6 , which is notably high in this model. This long-lasting and significant antibody response represents a desired characteristic given that the usual antibody kinetics is to start decreasing 2 weeks post-boost [63]. Following a second boost on day 140, titers rapidly returned to their peak levels (Figure 4A-C). Consistent with the single immunization titers, the 250 mg/mL MnGp gel outperformed the AddaVax-adjuvanted cohort, with boosting resulting in significantly higher total IgG, IgG1, and IgG2c (Figure 4 A-C) titers throughout most of the time course. Similarly, the 250 mg/mL MnGp gel elicited significantly higher titers across all measured subtypes compared to the cGAMP-adjuvanted cohort (Figure 4A-C). Thus, when compared to both another depot-forming adjuvant system (MF59) and cGAS-STING-targeting adjuvant (cGAMP), the MnGp gel demonstrates significant promise in humoral immunity alone. The addition of cGAMP did not significantly increase the humoral response, across a range of cGAMP doses (Figure S6), suggesting that MnGp might saturates local cGAS-STING signaling. Consequently, mice immunized with the MnGp-cGAMP combination were not included in the subsequent analysis.



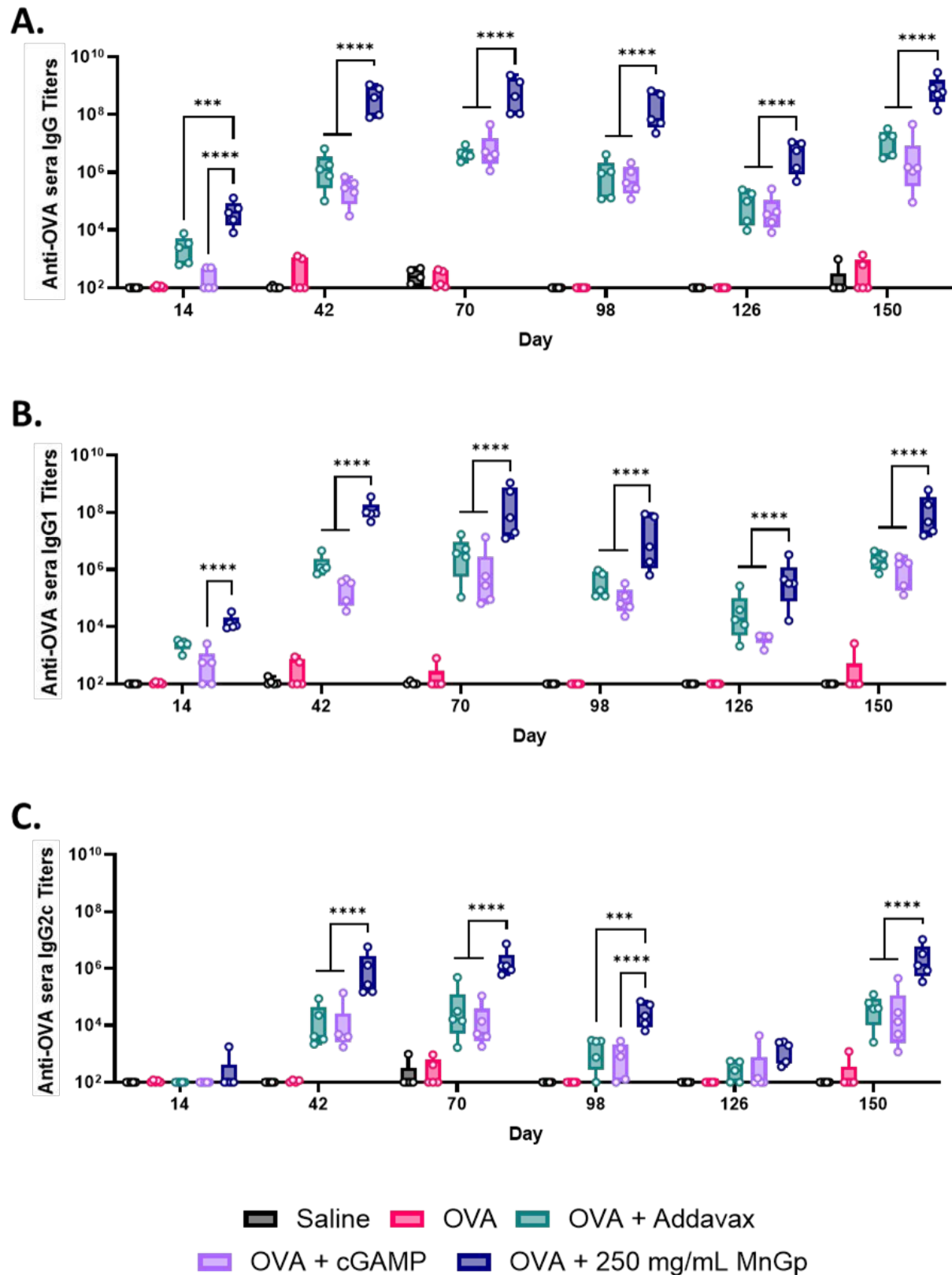


Figure 4. OVA-specific serum antibody titers following prime-boost-boost immunization schedule. C57BL/6 mice ($n = 5$) were immunized intramuscularly on days 0, 28, and 140 with saline, unadjuvanted OVA, OVA + Addavax, OVA + cGAMP, or OVA + 250 mg/mL MnGp. Sera were collected at the indicated timepoints and assessed for OVA-specific (A) total IgG, (B) IgG1 and (C) IgG2c titers via ELISA. Data is presented as median \pm range. Statistical significance is presented as $*p < 0.05$,



364 ** $p < 0.01$, *** $p < 0.001$, and **** $p < 0.0001$ for an ordinary two-way ANOVA with Tukey's multiple comparisons test.
365 Absence of statistical symbols indicates non-significant differences.

366 *Cellular Response to Optimal OVA-Loaded MnGp Gel Vaccine*

368 Cellular responses to vaccines are critical for durable protection, control of reinfection, and defense against
369 pathogens when antibodies are insufficient. In addition to the humoral response and their neutralizing activity, the
370 protection against smallpox acquired by vaccination has been linked to cellular immunity, primarily through CD4⁺ and CD8⁺
371 T cells. Those virus-specific T cells are responsible for clearing the initial infection, with robust memory populations
372 persisting for decades and controlling the early stages of the infection.[64, 65] Thus, we sought to profile the specific
373 immune phenotypes associated with sequential immunization with the MnGp gel vaccine formulation.

374 After the antigen recall of splenocytes, at day 151 and after following a prime-boost-boost immunization schedule
375 on days 0, 28, and 140; a trend of high IL-2-producing-cells and significant higher number of IFN- γ -secreting cells (Figure
376 5AB) were observed in mice of the MnGp vaccinated cohort compared to all other cohorts. A similar result was observed,
377 with significantly higher levels of IL-2 and IFN- γ from splenocytes of mice vaccinated with MnGp (Figure S8A, B). IFN- γ and
378 IL-2 are integral cytokines in T cell responses; particularly, Th1-like responses, driving antigen presenting cell (APC)
379 activation, Th1 differentiation, and T cell proliferation.[66] Therefore, the splenocyte restimulation data indicates that the
380 250 mg/mL MnGp gel is an ideal formulation for eliciting Th1 responses compared to more conventional adjuvant systems,
381 consistent with the IgG2c responses (Figure 3C, 4C).

367
368
369
370
371
372
373
374
375
376
377
378
379
380
381
This article is licensed under a Creative Commons Attribution-NonCommercial 3.0 Unported Licence.
Downloaded on 4/21/2026 11:06 AM.
Open Access Article. Published on 20 April 2026. Downloaded from www.rsc.org on 04/21/2026 11:06 AM.
This article is licensed under a Creative Commons Attribution-NonCommercial 3.0 Unported Licence.



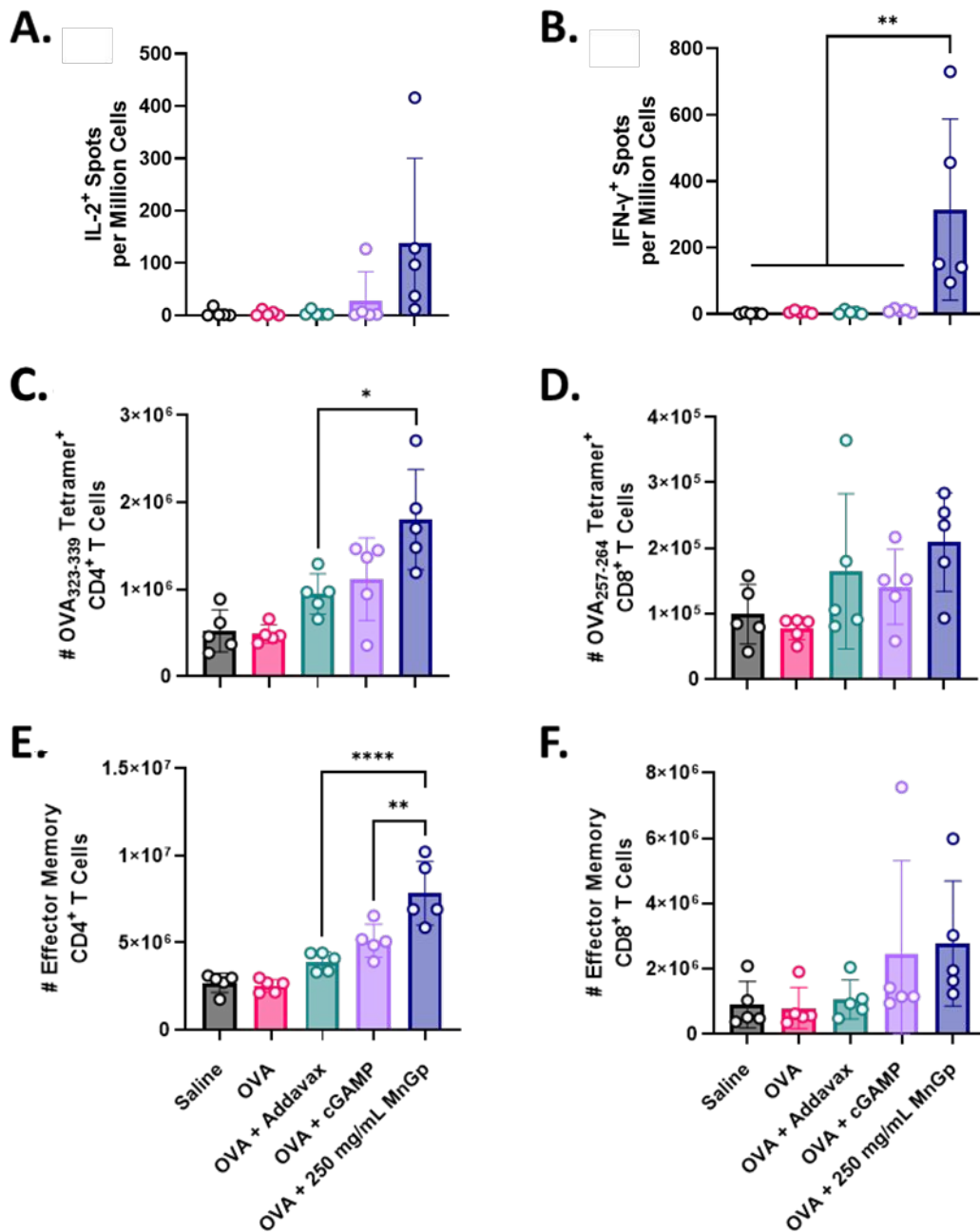


Figure 5. Antigen recall of splenocytes following a prime-boost-boost immunization schedule. C57BL/6 mice ($n = 5$) were immunized intramuscularly on days 0, 28, and 140 with saline, unadjuvanted OVA, OVA + Addavax, OVA + cGAMP, or OVA + 250 mg/mL MnGp. On day 151, splenocytes were collected and re-stimulated with OVA for 36 hours. ELISPOTs were performed to measure (A) IL-2-secreting cells and (B) IFN- γ -secreting cells. Flow cytometry was performed to quantify (C) OVA-specific CD4⁺ T cells, (D) OVA-specific CD8⁺ T cells, (E) effector memory CD4⁺ T cells (CD4⁺CD44⁺CD62L⁻) and (F) effector memory CD8⁺ T cells (CD4⁺CD44⁺CD62L⁻). Data is presented as mean \pm standard deviation. Statistical significance is presented as * $p < 0.05$, ** $p < 0.01$, and **** $p < 0.0001$ for ordinary two-way ANOVA with Tukey's multiple comparisons test. Absence of statistical symbols indicates non-significant differences.



382

383

384

385

386

387

388

389

390

391

When analyzed by flow cytometry, mice immunized with MnGp exhibited elevated OVA-specific CD4⁺ and CD8⁺ T cells in spleen with the OVA-specific CD4⁺ T cell counts significantly higher than those in mice immunized with AddaVax (Figure 5CD). The evaluation of the memory phenotype of T cells showed significantly higher effector memory (CD44⁺CD62L⁻) CD4⁺ T cells in the spleen of mice immunized with MnGp compared to mice immunized with AddaVax or cGAMP, however the number of effector memory CD8⁺ T cells remained similar between them (Figure 5EF). Together, these data likely explain the previous IFN- γ and IL-2 ELISPOT and ELISA data (Figure 5), as effector memory CD4⁺ T cells are primarily responsible for rapid mobilization of the immune response upon exposure to their cognate antigen.[67] On the other hand, the number of central memory CD4⁺ and CD8⁺ T cells (CD44⁺CD62L⁺) were similar to our Addavax or cGAMP controls (Figure S8CD). In addition to T cells, B cell phenotypes were additionally profiled. Immunization with the 250 mg/mL MnGp gel induced greater counts of both splenic germinal center (GC; CD19⁺GL7⁺CD38⁻) and activated (CD19⁺GL7⁻CD38⁺) B cells compared to AddaVax and cGAMP, although these differences were not significant (Figure S9AB), although there might be a difference if, in the future, we quantify the GC B cells in the draining lymph node of mice immunized with MnGp. Overall, these data align with the properties of the MnGp gel, that compared to AddaVax and cGAMP, the gel forms a highly immunogenic depot that continually releases antigen and Mn, resulting in continuous immune stimulation and maintenance of effector-like phenotypes.

Immunization of MnGp Gel in an aged mice model

To assess the potential of this vaccine platform in immunocompromised populations, we immunized aged mice, a high-risk group with reduced immune responsiveness. We immunized 18-month-old C57BL/6 mice (i.e. elderly) with MnGp and evaluated the immune response. In this population, the antigen-specific IgG and IgG1 sera titers from mice immunized with MnGp were significantly higher than the titers reached with the Addavax group (Figure 6AB). On the other hand, IgG2c titers remained similar in both groups (Figure 6C). Following antigen recall, splenocytes from aged mice immunized with MnGp showed a non-significant trend toward increased IL-2 production, with similar trends observed for IFN- γ and IL-4. Cytokine levels were generally higher than those in the non-adjuvanted group, but comparable to responses elicited by AddaVax (Figure 6DE and Figure S10).



In general, the immune response induced by MnGp in aged mice was robust, inducing a sustained antigen-specific IgG and IgG1 titers (around 10^6) and detectable T cell responses that indicate the presence of Th1 and Th2 responses in those mice. It is important to highlight that the robust immune response induced by MnGp is a good indicator of the potential of this platform for a high-risk population vaccine, given that other adjuvant systems like cGAMP have only induced IgG titers of the order of around 10^4 ; in addition, cGAMP induce a practically null presence of IL-2 and IFN- γ cellular responses in aged mice [49].

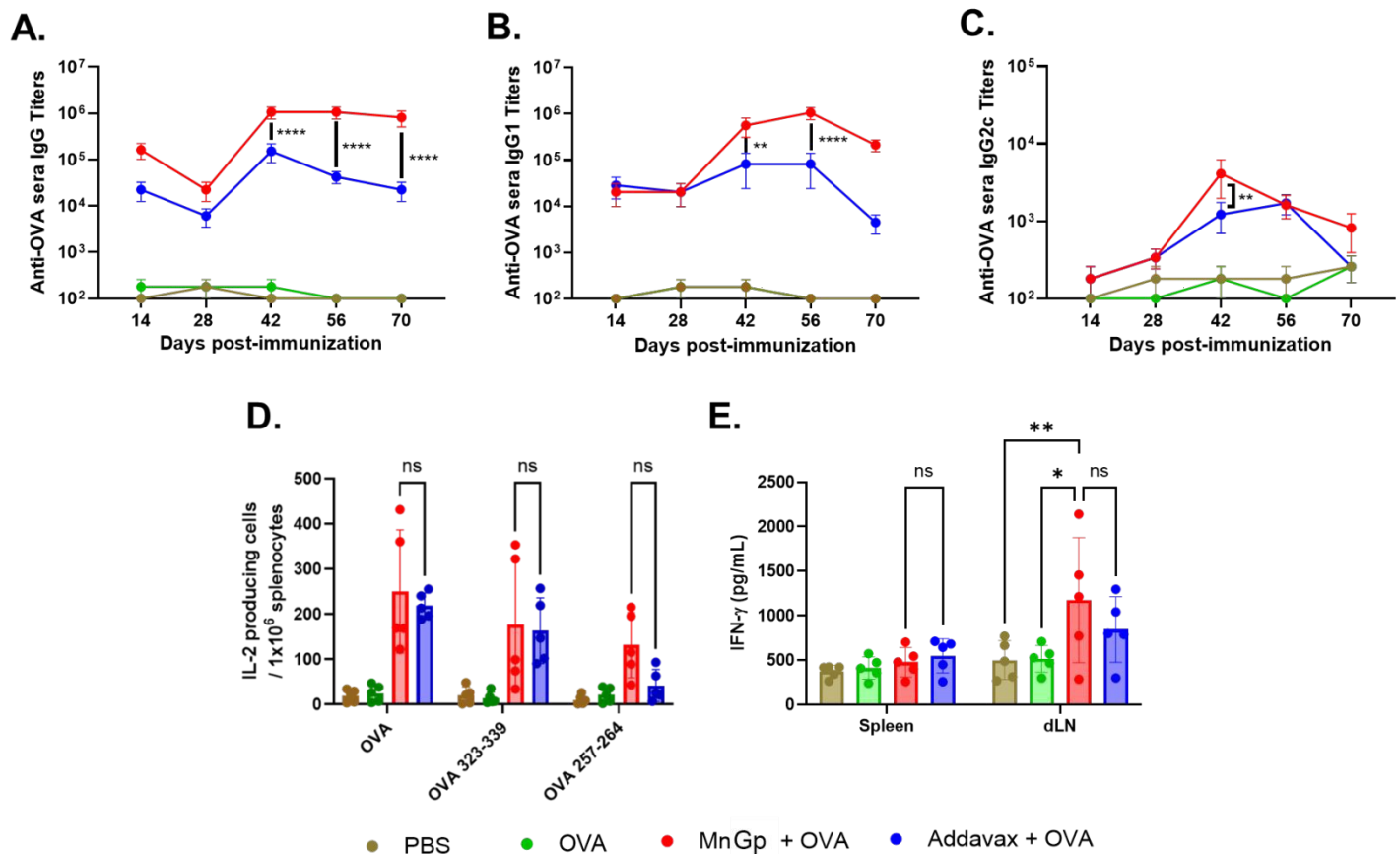


Figure 6 Humoral and cellular responses in aged mice immunized with MnGp. C57BL/6 18-month-old mice ($n = 5$) were immunized intramuscularly on days 0, 28 and 77 with PBS, unadjuvanted OVA, MnGp (250 mg/mL) + OVA or Addavax + OVA. **(A)** Sera IgG, **(B)** IgG1 and **(C)** IgG2c were measured at different timepoints. **(D)** IL-2 producing cells in spleen and **(E)** IFN- γ production from splenocytes and dLN cells harvested on day 84 after a re-stimulation with OVA and OVA peptide. Data is presented as mean \pm standard deviation. Statistical significance is presented as * $p < 0.05$, ** $p < 0.01$, and *** $p < 0.0001$ for an ordinary two-way ANOVA with Tukey's multiple comparisons test.



436 *Use of MnGp Gel for a Pox Virus Vaccine*

437 Mice immunized with MnGp and B5R exhibited high levels of B5R-specific antibody titers for up to 8 weeks post-
438 vaccination. IgG, IgG1 and IgG2c sera titers from mice immunized with MnGp were significantly higher than the titers
439 reached with the Addavax group (Figure 7A-C), demonstrating the strong immunogenicity induced by this formulation and
440 highlighting the presence of Th1 and Th2 responses versus B5R in mice. After the challenge, the immunization with MnGp
441 was the only condition that achieved full (100%) protection versus vaccinia virus, where Addavax reached 80% of final
442 survival while the rest of the groups succumbed to infection (Figure 7D). A similar protection pattern was found after
443 analyzing the weight loss curves and the clinical scores, where in general, a better (but not significant) protection pattern
444 was observed in mice immunized with MnGp compared with Addavax (Figure S11AB).

445 This promising result aligned with the previous immunological characterization, in which we observed a long-
446 lasting antibody response and a strong cellular immune response, suggesting that those mechanisms might be involved in
447 the full protection observed in mice vaccinated with MnGp. In general, the efficacy of the current FDA-approved
448 monkeypox vaccines is between 75-85% [68], therefore, would be interesting to keep investigating the potential of MnGp
449 as a vaccine platform against *Orthopox* viruses.



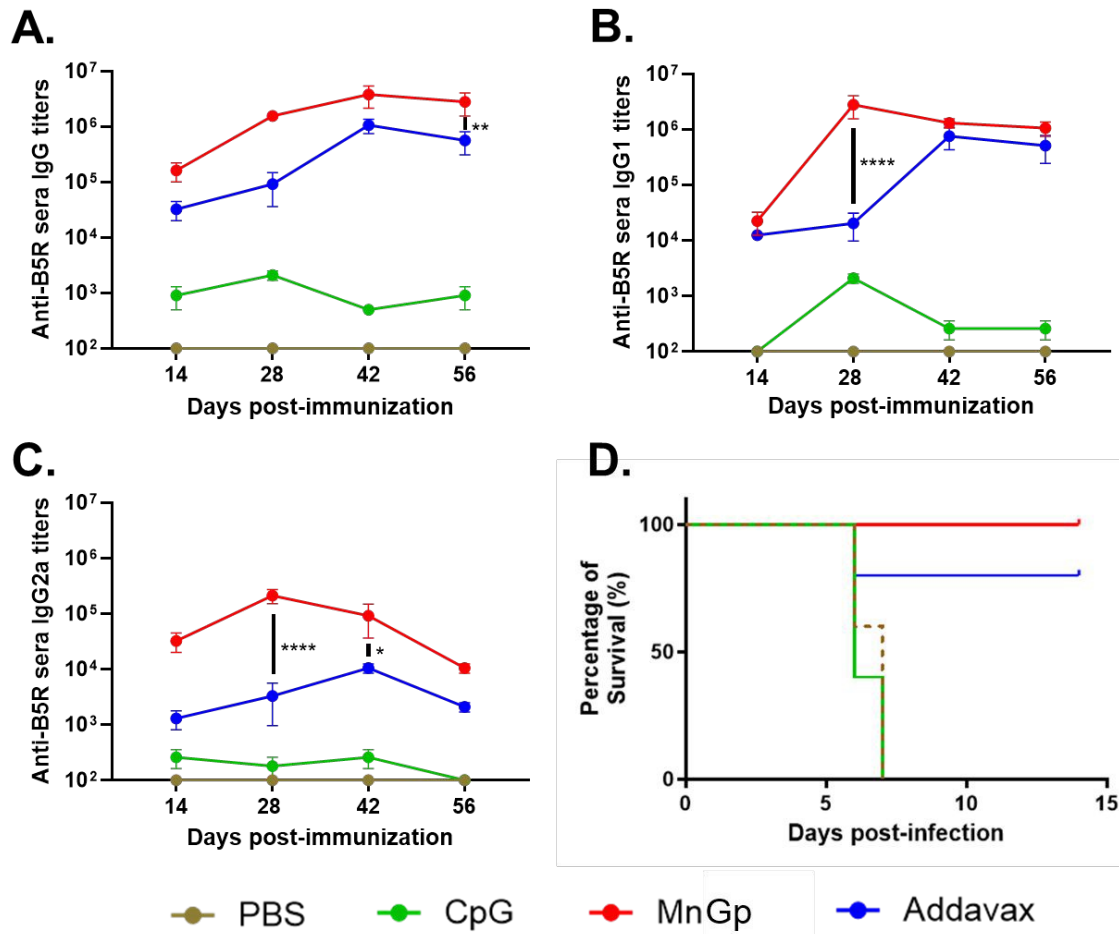


Figure 7. IgG, IgG1, IgG2a sera titers and survival from mice immunized with MnGp + B5R and challenged with vaccinia virus. BALB/c mice ($n = 10$) were immunized intramuscularly on days 0 and 28 with PBS, CpG + B5R, MnGp (250 mg/mL) + B5R or Addavax + B5R. On day 56 the mice were challenged with vaccinia virus. **(A)** Sera IgG, **(B)** IgG1 and **(C)** IgG2a titers at different timepoints. **(D)** Survival of mice after challenge. Data is presented as mean \pm standard deviation. Statistical significance is presented as * $p < 0.05$, ** $p < 0.01$, and **** $p < 0.0001$ for an ordinary two-way ANOVA with Tukey's multiple comparisons test.

Conclusion

The present work described the synthesis, characterization, and administration of a novel Mn-based gel for vaccine applications. The MnGp gel was fabricated via a scalable and facile sonication method, and gels of varying MnGp content displayed tunable release of the model antigen OVA over the course of a week. MnGp exhibited *in vitro* activation of dendritic cells, resulting in elevated type I interferon secretion and increased expression of co-stimulatory markers. Immunization of MnGp with OVA elicited a strong immune response as a single-dose or prime-boost vaccine, showing sustained antibody titers and a robust T cell response, outperforming AddaVax, an analog to the FDA-approved adjuvant MF59. MnGp displayed promising immunological features in aged mice, inducing sustained IgG titers and the presence of



specific T cells. Finally, used as a vaccine platform against the *Orthopoxvirus* vaccinia, MnGp was able to produce B5R-specific antibodies and protect all the mice after the viral challenge. Overall, this MnGp platform represents a highly efficacious strategy for improving and prolonging both the humoral and cellular immune responses to subunit vaccines.

Acknowledgements

This work was supported, in part, by National Institutes of Health (NIH) NIAID R01AI147497 (PI: Ainslie). This work was performed in part at the Chapel Hill Analytical and Nanofabrication Laboratory, CHANL, a member of the North Carolina Research Triangle Nanotechnology Network, RTNN, which is supported by the National Science Foundation, Grant ECCS-2025064, as part of the National Nanotechnology Coordinated Infrastructure, NNCI. The UNC Flow Cytometry Core Facility (RRID: SCR_019170) is supported in part by P30 CA016086 Cancer Center Core Support Grant to the UNC Lineberger Comprehensive Cancer Center, the North Carolina Biotech Center Institutional Support Grant 2017-IDG-1025, and by the National Institutes of Health 1UM2AI30836-01. Graphics created with BioRender.com. The content is solely the responsibility of the authors and does not necessarily represent the official views of the National Institutes of Health.

Author Contributions

J.A.R., M.J.I. and S.A.E. synthesized and characterized the materials. L.O.P., M.J.I., S.A.E., J.A.R., D.D.M., C.T.M., N.R.L., D.A.H., E.S.P., R.N.S. and W.J.P. participated in investigation and data acquisition. M.J.I. primarily curated and organized data. M.J.I., L.O.P. and S.A.E. drafted the original manuscript and figures. All authors participated in manuscript revision. K.M.A. and E.M.B. conceptualized and supervised the research, and K.M.A. secured funding resources.

Conflict of Interest Statement

There are no conflicts to declare. E.M.B., K.M.A., J.A.R., M.J.I., and S.A.E. filed a provisional patent with the University of North Carolina at Chapel Hill (U.S. Provisional Patent Application No. 63/714,626).

493

494 **Data Availability Statement**

495 The data that support the findings of this study are available from the corresponding author upon reasonable request.

496 **Ethical Statement**497 All animal procedures were performed in accordance with the Guidelines for Care and Use of Laboratory Animals
498 of University of North Carolina at Chapel Hill and approved by UNC Institutional Animal Care and Use Committee.499 **References:**

- 500
-
- 501 1. Rodrigues, C.M.C. and S.A. Plotkin,
- Impact of Vaccines; Health, Economic and Social*
-
- 502
- Perspectives*
- . Front Microbiol, 2020.
- 11**
- : p. 1526.
-
- 503 2. Roush, S.W., T.V. Murphy, and G. Vaccine-Preventable Disease Table Working,
- Historical*
-
- 504
- comparisons of morbidity and mortality for vaccine-preventable diseases in the United States*
- .
-
- 505 JAMA, 2007.
- 298**
- (18): p. 2155-63.
-
- 506 3. Shchelkunov, S.N.,
- An increasing danger of zoonotic orthopoxvirus infections*
- . PLoS Pathog,
-
- 507 2013.
- 9**
- (12): p. e1003756.
-
- 508 4. Di Giulio, D.B. and P.B. Eckburg,
- Human monkeypox: an emerging zoonosis*
- . Lancet Infect Dis,
-
- 509 2004.
- 4**
- (1): p. 15-25.
-
- 510 5. Keikha, M., M. Zandhaghighi, and S. Shahraki Zahedani,
- Death-associated with human*
-
- 511
- monkeypox outbreak 2022: the current perspectives - correspondence*
- . Int J Surg, 2023.
- 109**
- (6):
-
- 512 p. 1806-1807.
-
- 513 6. Lum, F.M., et al.,
- Monkeypox: disease epidemiology, host immunity and clinical interventions*
- .
-
- 514 Nat Rev Immunol, 2022.
- 22**
- (10): p. 597-613.
-
- 515 7. Ai-ris, Y.C., et al.,
- Decline of Mpox Antibody responses after modified vaccinia Ankara–Bavarian*
-
- 516
- Nordic vaccination*
- . JAMA, 2024.
- 332**
- (19): p. 1669-1672.
-
- 517 8. Chakraborty, S., et al.,
- Monkeypox vaccines and vaccination strategies: Current knowledge and*
-
- 518
- advances. An update - Correspondence*
- . Int J Surg, 2022.
- 105**
- : p. 106869.
-
- 519 9. Mitjà, O., et al.,
- Mpox in people with advanced HIV infection: a global case series*
- . The Lancet,
-
- 520 2023.
- 401**
- (10380): p. 939-949.
-
- 521 10. Ortiz-Saavedra, B., et al.,
- Epidemiologic situation of HIV and monkeypox coinfection: a*
-
- 522
- systematic review*
- . Vaccines, 2023.
- 11**
- (2): p. 246.
-
- 523 11. Kelly, J.D., et al.,
- Incidence of Severe COVID-19 Illness Following Vaccination and Booster With*
-
- 524
- BNT162b2, mRNA-1273, and Ad26.COVS Vaccines*
- . JAMA, 2022.
- 328**
- (14): p. 1427-1437.
-
- 525 12. Lin, D.Y., et al.,
- Effectiveness of Covid-19 Vaccines over a 9-Month Period in North Carolina*
- . N
-
- 526 Engl J Med, 2022.
- 386**
- (10): p. 933-941.
-
- 527 13. Polack, F.P., et al.,
- Safety and Efficacy of the BNT162b2 mRNA Covid-19 Vaccine*
- . N Engl J
-
- 528 Med, 2020.
- 383**
- (27): p. 2603-2615.
-
- 529 14. Uddin, M.N. and M.A. Roni,
- Challenges of Storage and Stability of mRNA-Based COVID-19*
-
- 530
- Vaccines*
- . Vaccines (Basel), 2021.
- 9**
- (9).
-
- 531 15. Sutton, N., et al.,
- Comparing reactogenicity of COVID-19 vaccines: a systematic review and*
-
- 532
- meta-analysis*
- . Expert Rev Vaccines, 2022.
- 21**
- (9): p. 1301-1318.
-
- 533 16. Minor, P.D.,
- Live attenuated vaccines: Historical successes and current challenges*
- . Virology,
-
- 534 2015.
- 479-480**
- : p. 379-92.
-
- 535 17. Plotkin, S.,
- History of vaccination*
- . Proc Natl Acad Sci U S A, 2014.
- 111**
- (34): p. 12283-7.

This article is licensed under a Creative Commons Attribution-NonCommercial 3.0 Unported Licence.
11:11:00 AM
21/2024

18. Kyriakidis, N.C., et al., *SARS-CoV-2 vaccines strategies: a comprehensive review of phase 3 candidates*. NPJ Vaccines, 2021. **6**(1): p. 28.
19. Reed, S.G., M.T. Orr, and C.B. Fox, *Key roles of adjuvants in modern vaccines*. Nat Med, 2013. **19**(12): p. 1597-608.
20. Lindblad, E.B., *Aluminium compounds for use in vaccines*. Immunol Cell Biol, 2004. **82**(5): p. 497-505.
21. Pulendran, B., S.A. P, and D.T. O'Hagan, *Emerging concepts in the science of vaccine adjuvants*. Nat Rev Drug Discov, 2021. **20**(6): p. 454-475.
22. Alebrahim-Dehkordi, E., et al., *T helper type (Th1/Th2) responses to SARS-CoV-2 and influenza A (H1N1) virus: From cytokines produced to immune responses*. Transpl Immunol, 2022. **70**: p. 101495.
23. Knutson, K.L. and M.L. Disis, *Tumor antigen-specific T helper cells in cancer immunity and immunotherapy*. Cancer Immunol Immunother, 2005. **54**(8): p. 721-8.
24. Didierlaurent, A.M., et al., *AS04, an aluminum salt- and TLR4 agonist-based adjuvant system, induces a transient localized innate immune response leading to enhanced adaptive immunity*. J Immunol, 2009. **183**(10): p. 6186-97.
25. Ko, E.J. and S.M. Kang, *Immunology and efficacy of MF59-adjuvanted vaccines*. Hum Vaccin Immunother, 2018. **14**(12): p. 3041-3045.
26. Bechtold, V., et al., *Functional and epigenetic changes in monocytes from adults immunized with an AS01-adjuvanted vaccine*. Sci Transl Med, 2024. **16**(758): p. eadl3381.
27. Martins, K.A., S. Bavari, and A.M. Salazar, *Vaccine adjuvant uses of poly-IC and derivatives*. Expert Rev Vaccines, 2015. **14**(3): p. 447-59.
28. Bode, C., et al., *CpG DNA as a vaccine adjuvant*. Expert Rev Vaccines, 2011. **10**(4): p. 499-511.
29. Li, X.D., et al., *Pivotal roles of cGAS-cGAMP signaling in antiviral defense and immune adjuvant effects*. Science, 2013. **341**(6152): p. 1390-4.
30. Lv, M., et al., *Manganese is critical for antitumor immune responses via cGAS-STING and improves the efficacy of clinical immunotherapy*. Cell Res, 2020. **30**(11): p. 966-979.
31. Wang, C., et al., *Manganese Increases the Sensitivity of the cGAS-STING Pathway for Double-Stranded DNA and Is Required for the Host Defense against DNA Viruses*. Immunity, 2018. **48**(4): p. 675-687 e7.
32. Zhang, R., et al., *Manganese salts function as potent adjuvants*. Cell Mol Immunol, 2021. **18**(5): p. 1222-1234.
33. Zhao, Z., et al., *Mn(2+) Directly Activates cGAS and Structural Analysis Suggests Mn(2+) Induces a Noncanonical Catalytic Synthesis of 2'3'-cGAMP*. Cell Rep, 2020. **32**(7): p. 108053.
34. Hopfner, K.P. and V. Hornung, *Molecular mechanisms and cellular functions of cGAS-STING signalling*. Nat Rev Mol Cell Biol, 2020. **21**(9): p. 501-521.
35. Fan, N., et al., *Manganese-coordinated mRNA vaccines with enhanced mRNA expression and immunogenicity induce robust immune responses against SARS-CoV-2 variants*. Sci Adv, 2022. **8**(51): p. eabq3500.
36. Aikins, M.E., et al., *STING-activating cyclic dinucleotide-manganese nanoparticles evoke robust immunity against acute myeloid leukemia*. J Control Release, 2024. **368**: p. 768-779.
37. Gao, Z.L., et al., *Orchestrated Cytosolic Delivery of Antigen and Adjuvant by Manganese Ion-Coordinated Nanovaccine for Enhanced Cancer Immunotherapy*. Nano Lett, 2023. **23**(5): p. 1904-1913.
38. Hou, L., et al., *Manganese-Based Nanoactivator Optimizes Cancer Immunotherapy via Enhancing Innate Immunity*. ACS Nano, 2020. **14**(4): p. 3927-3940.
39. Ma, Q., et al., *Manganese-based nanoadjuvants for enhancement of immune effect of DNA vaccines*. Front Bioeng Biotechnol, 2022. **10**: p. 1053872.
40. OuYang, X., et al., *Manganese-Based Nanoparticle Vaccine for Combating Fatal Bacterial Pneumonia*. Adv Mater, 2023. **35**(51): p. e2304514.
41. Qiao, N., et al., *A MnAl double adjuvant nanovaccine to induce strong humoral and cellular immune responses*. J Control Release, 2023. **358**: p. 190-203.



42. Awate, S., L.A. Babiuk, and G. Mutwiri, *Mechanisms of action of adjuvants*. Front Immunol, 2013. **4**: p. 114.
43. Li, J. and D.J. Mooney, *Designing hydrogels for controlled drug delivery*. Nat Rev Mater, 2016. **1**(12).
44. Roque, J.A., 3rd, et al., *Enhancement of subunit vaccine delivery with zinc-carnosine coordination polymer through the addition of mannan*. Int J Pharm, 2024. **656**: p. 124076.
45. Lutz, M.B., et al., *An advanced culture method for generating large quantities of highly pure dendritic cells from mouse bone marrow*. J Immunol Methods, 1999. **223**(1): p. 77-92.
46. Jin, D. and J. Sprent, *GM-CSF Culture Revisited: Preparation of Bulk Populations of Highly Pure Dendritic Cells from Mouse Bone Marrow*. J Immunol, 2018. **201**(10): p. 3129-3139.
47. Batty, C.J., et al., *Vinyl Sulfone-functionalized Acetalated Dextran Microparticles as a Subunit Broadly Acting Influenza Vaccine*. AAPS J, 2023. **25**(1): p. 22.
48. Shchelkunov, S.N., et al., *Adaptive Immune Response to Vaccinia Virus L1VP Infection of BALB/c Mice and Protection against Lethal Reinfection with Cowpox Virus*. Viruses, 2021. **13**(8).
49. Hendy, D.A., et al., *Immunogenicity of an adjuvanted broadly active influenza vaccine in immunocompromised and diverse populations*. Bioeng Transl Med, 2024. **9**(2): p. e10634.
50. Eckshtain-Levi, M., et al., *Metal-Organic Coordination Polymer for Delivery of a Subunit Broadly Acting Influenza Vaccine*. ACS Appl Mater Interfaces, 2022. **14**(25): p. 28548-28558.
51. Frey, A., J. Di Canzio, and D. Zurakowski, *A statistically defined endpoint titer determination method for immunoassays*. J Immunol Methods, 1998. **221**(1-2): p. 35-41.
52. Zhang, W., et al., *The use of injectable sonication-induced silk hydrogel for VEGF(165) and BMP-2 delivery for elevation of the maxillary sinus floor*. Biomaterials, 2011. **32**(35): p. 9415-24.
53. Wang, X., et al., *Sonication-induced gelation of silk fibroin for cell encapsulation*. Biomaterials, 2008. **29**(8): p. 1054-64.
54. Pramanik, A., et al., *Sonication-Induced, Solvent-Selective Gelation of a 1,8-Naphthalimide-Conjugated Amide: Structural Insights and Pollutant Removal Applications*. ACS Omega, 2021. **6**(48): p. 32722-32729.
55. Tong, J., et al., *Physically crosslinked chitosan/alpha-glycerophosphate hydrogels enhanced by surface-modified cyclodextrin: An efficient strategy for controlled drug release*. Int J Biol Macromol, 2024. **283**(Pt 1): p. 137163.
56. Lee, M.K., et al., *Cryoprotectants for freeze drying of drug nano-suspensions: effect of freezing rate*. J Pharm Sci, 2009. **98**(12): p. 4808-17.
57. Chen, M.H., et al., *Methods To Assess Shear-Thinning Hydrogels for Application As Injectable Biomaterials*. ACS Biomater Sci Eng, 2017. **3**(12): p. 3146-3160.
58. Yan, C., et al., *Injectable solid hydrogel: mechanism of shear-thinning and immediate recovery of injectable beta-hairpin peptide hydrogels*. Soft Matter, 2010. **6**(20): p. 5143-5156.
59. Wang-Bishop, L., et al., *Potent STING activation stimulates immunogenic cell death to enhance antitumor immunity in neuroblastoma*. J Immunother Cancer, 2020. **8**(1).
60. Sinigaglia, F., D. D'Ambrosio, and L. Rogge, *Type I interferons and the Th1/Th2 paradigm*. Dev Comp Immunol, 1999. **23**(7-8): p. 657-63.
61. Nazeri, S., et al., *Measuring of IgG2c isotype instead of IgG2a in immunized C57BL/6 mice with Plasmodium vivax TRAP as a subunit vaccine candidate in order to correct interpretation of Th1 versus Th2 immune response*. Exp Parasitol, 2020. **216**: p. 107944.
62. Collins, A.M., *IgG subclass co-expression brings harmony to the quartet model of murine IgG function*. Immunol Cell Biol, 2016. **94**(10): p. 949-954.
63. Hauge, S., et al., *Quality and kinetics of the antibody response in mice after three different low-dose influenza virus vaccination strategies*. Clin Vaccine Immunol, 2007. **14**(8): p. 978-83.
64. Kunasekaran, M.P., et al., *Evidence for Residual Immunity to Smallpox After Vaccination and Implications for Re-emergence*. Mil Med, 2019. **184**(11-12): p. e668-e679.
65. Gordon, S.N., et al., *Smallpox vaccine safety is dependent on T cells and not B cells*. J Infect Dis, 2011. **203**(8): p. 1043-53.
66. Romagnani, S., *Th1/Th2 cells*. Inflamm Bowel Dis, 1999. **5**(4): p. 285-94.

588
589
590
591
592
593
594
595
596
597
598
599
600
601
602
603
604
605
606
607
608
609
610
611
612
613
614
615
616
617
618
619
620
621
622
623
624
625
626
627
628
629
630
631
632
633
634
635
636
637
638
639



This article is licensed under a Creative Commons Attribution-NonCommercial 3.0 Unported License.

Nanoscale Accepted Manuscript

- 640 67. Kunzli, M. and D. Masopust, *CD4(+) T cell memory*. *Nat Immunol*, 2023. **24**(6): p. 903-914.
641 68. Pischel, L., et al., *Vaccine effectiveness of 3rd generation mpox vaccines against mpox and*
642 *disease severity: A systematic review and meta-analysis*. *Vaccine*, 2024. **42**(25): p. 126053.

643

644

645

646

647

648

649

650

651

652

653

654

655

656

657

658

659

660

661

662

663

664

665

666

667

668

669

670

671

672

673

674

675

676

677

678

679

680

681

682

683

684

685

686

687

688

689

690

691

692

Open Access Article. Published on 20 April 2026. Downloaded on 4/21/2026 1:11:06 AM.
This article is licensed under a Creative Commons Attribution-NonCommercial 3.0 Unported Licence.



Data availability

The data supporting this study will be available through the NIH NIAID Collaborative Influenza Vaccine Innovation Centers (CIVIC) database. Access can be obtained via the database portal, and additional details are available from the corresponding author upon reasonable request.

